

A MODIFIED THERMAL VISCOPLASTIC CONSTITUTIVE LAW INVOLVING THE EFFECT OF TEMPERATURE RISE RATE*

Huang Chenguang Duan Zhuping

(LNM, Institute of Mechanics, Chinese Academy of Sciences, Beijing 100080, China)

ABSTRACT At high temperature rise rate, the mechanical properties of 10 # steel were determined experimentally in a very wide range of temperature and strain rates. A new constitutive relationship was put forward, which can fit with the experimental results and describe various phenomena observed in our experiments. Meanwhile, some interesting characteristics about the temperature rise rate, strain and strain rate hardening and thermal softening are also shown in this paper. Finally, the reliability of the constitutive law and the correctness of the constitutive parameters were verified by comparing the calculation results with the experimental data.

KEY WORDS constitutive law, strain rate, temperature rise rate

I. INTRODUCTION

The construction and the constitutive law of target materials were very important and impending in the investigation of deformation and failure of a target induced by a laser beam. In general, when the metal target is irradiated by a laser beam, its strain rate and temperature rise rate ranges are 10^3 K/s - 10^7 K/s, 10^{-1} s $^{-1}$ - 10^3 s $^{-1}$, respectively, depending on the laser power density. So, it is necessary for the new constitutive law to be able to bear the effects of the temperature rise rate and strain rate, be applicable in a wide temperature range, and have a reliable physical basis and a simple mathematical form.

Although the constitutive equation that can meet the above requirements has hardly been reported, many researchers have contributed their efforts to an understanding of the effects of the strain rate, temperature etc. on the deformation mechanism and properties of materials. Frost and Ashby^[1] presented some key factors that control the deformation of general metal materials in different thermal and loading conditions, and put forward several mathematical models to depict these different deformation mechanisms. Anand et al.^[2] and Chan^[3] investigated experimentally and theoretically the mechanical properties and constitutive law of several materials at different ambient temperatures under relatively lower strain and temperature rise rates, and obtained some systematic and important results. As to the effect of strain rate on the mechanical behaviors of materials, the experimental observations and theoretical analyses published by Armstrong, Klepaczko, Bodner et al.^[3-8] are of great value.

In this paper, 10 # steel, a kind of widely used low carbon structural steel, is selected as the

* This project is supported partly by The Laser Technology Field of National High Technology Plan and partly by Key-Grant of NNSF of China (No.19891180 - 4).

Received 3 August 1999.

material for investigation. In the second section, a set of experimental schemes is designed and implemented to obtain the macroscopic strain vs. stress relationship under different conditions of temperature, strain rate and temperature rise rate. In the third section, a new constitutive law is presented based on an analysis of the physical background of deformation and the test results of macroscopic mechanical behaviours, and the constitutive parameters are determined by a nonlinear fitting algorithm. In the last part, our investigation on the new constitutive law is reviewed.

II . EXPERIMENTAL SETUP AND RESULTS

Table 1 shows the element composition of 10 # steel. Metallographic microscopy and SEM observation of polished 10 # steel samples indicate that the perlite and ferrite are the main composite microstructures, with a small quantity of voids and impurities. Hot rolled 10 # steel bars are used in our experiments.

Table 1 The element composition of 10 # steel (Fe is not included)

element	C	Mn	Si	Cr	S
content(%)	0.09	0.47	0.25	0.10	0.04

In our experiment, several testing devices were adopted, including the Instron universal testing machine and the Gleeble 1500 provided by Beijing Institute of Electromechanics, and a new type of Split Hopkinson Tension Bar(SHTB) equipped in our laboratory. The ranges of temperature, strain rate and temperature rise rate output by these experimental devices are shown in the Table 2. The operation procedures and sample dimensions etc. are described in detail in Ref.[9].

Table 2 The ranges of temperature, strain rate and temperature rise rate output by main testing devices

device	strain rate(s^{-1})	temperature(K)	temperature rise rate(K/s)
Gleeble 1500	$10^{-4} - 10^0$	$T_{room} - T_{melt}$	$10^{-1} - 10^5$
SHTB + electric resistance furnace	$10^2 - 10^3$	800K	$10^{-1} - 10^0$
SHTB + large current heater	$10^2 - 10^3$	1300K	$10^1 - 10^3$

To gain and understand the macroscopic relationship among the flow stress and strain, strain rate, temperature and temperature rise rate, three types of mechanical testing were carried out.

2.1 Determination of Temperature Rise Rate Effect

(1) Samples were heated up to a certain temperature, such as 623K, by different heating rates of 7.3×10^{-2} , 2.3×10^{-1} , 1, 10, 100, 1000 Ks^{-1} , then, stretched to failure by Gleeble 1500. The histories of temperature, strain and stress were obtained by thermocouple sensors, quartz strain sensors and loadometers, which were connected with a personal computer. By varying the objective temperature from 623 K to 873 K, a similar procedure was repeated once again.

(2) Tensile samples were heated up to 623 K with different heating devices, the electric resistance furnace ($\dot{T} \approx 0.5 Ks^{-1}$) and the large power current heater ($\dot{T} \approx 100 Ks^{-1}$) and then impacted to breakage by SHTB.

Through these testing, the relationship between the flow stress and the temperature rise rate was

obtained, as shown in Fig.1. From this figure, it can be seen that the flow stress of 10 # steel is highly sensitive to the temperature rise rate, and the sensitivity increases with the rise of the objective temperature. It should be mentioned that there is a turning point (about 10^{-1} Ks^{-1}) in the curve. Only when the temperature rise rate of samples is lower than this value, will the dependence of flow stress on temperature rise rate become visible.

2.2 Effects of Temperature and Strain Rate

(1) When the temperature rise rate and objective temperature were fixed at 1000 Ks^{-1} and 623 K respectively, samples were stretched with the strain rates of $0.5, 0.05$ and 0.005 s^{-1} by the Gleeble 1500 testing machine. The objective temperature was varied from 300 K , to 873 K , 1072 K and 1273 K respectively, and the test was repeated after the signals output by various sensors were recorded.

(2) By the newly modified SHTB, samples were tested under different ambient temperatures, i.e., 300 K , 532 K , 623 K and 673 K , with the same temperature rise rate (0.5 Ks^{-1}) and strain rate ($2 \times 10^3 \text{ s}^{-1}$).

Figures 2 and 3 show the effect of temperature on the relationship between strain and stress under quasi-static and impacting loadings. Figures 4 and 5 show the dependence of flow stress of 10 # steel on the strain rate at different ambient temperatures. A common phenomenon is seen that the increase of temperature and the reduction of strain rate result in the decrease of the yielding stress, hardening modulus and ultimate tensile strength. However, a perplexing exception occurred at the temperature of 623 K and lower strain rate, that rules of thermal softening and strain rate hardening failed.

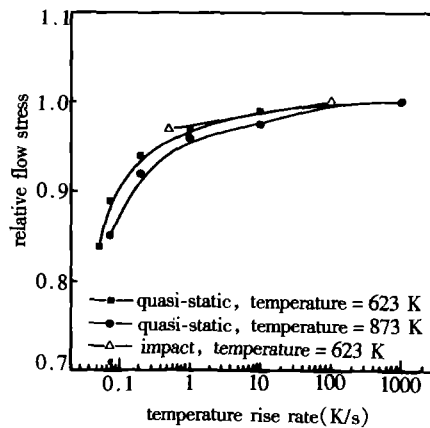


Fig.1 The effect of temperature rise rate to the flow stress of 10 # steel at the strain of 0.1.

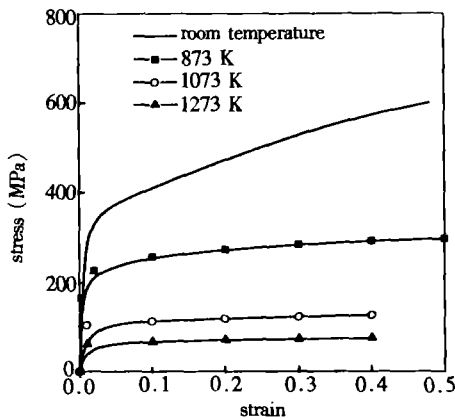


Fig.2 The strain-stress curves of 10 # steel at different temperatures under quasi-static loadings.

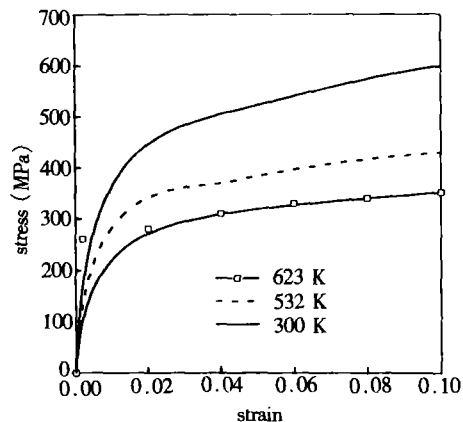


Fig.3 The stress strain relations of 10 # steel in impact loading with different temperatures.

Figure 6 shows the strain rate sensitivity of flow stress of 10 # steel at different temperatures. In general, the rate sensitivity is defined as:

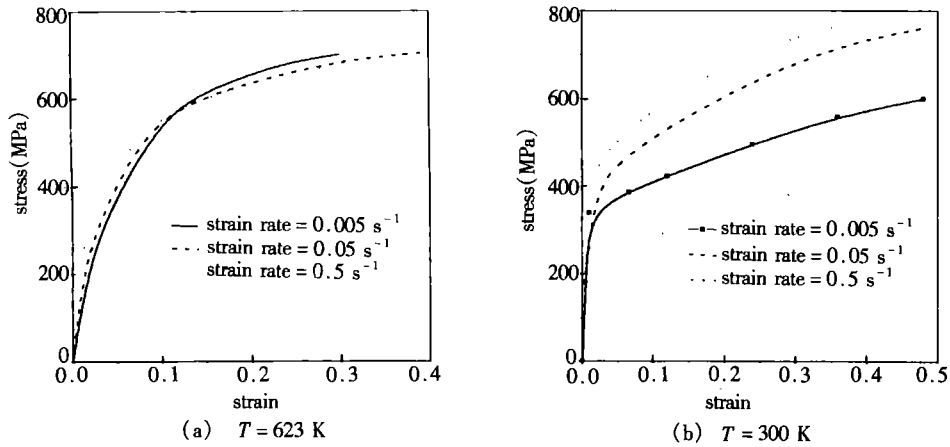


Fig.4 The stress-strain curves of 10 # steel in quasi-static condition.

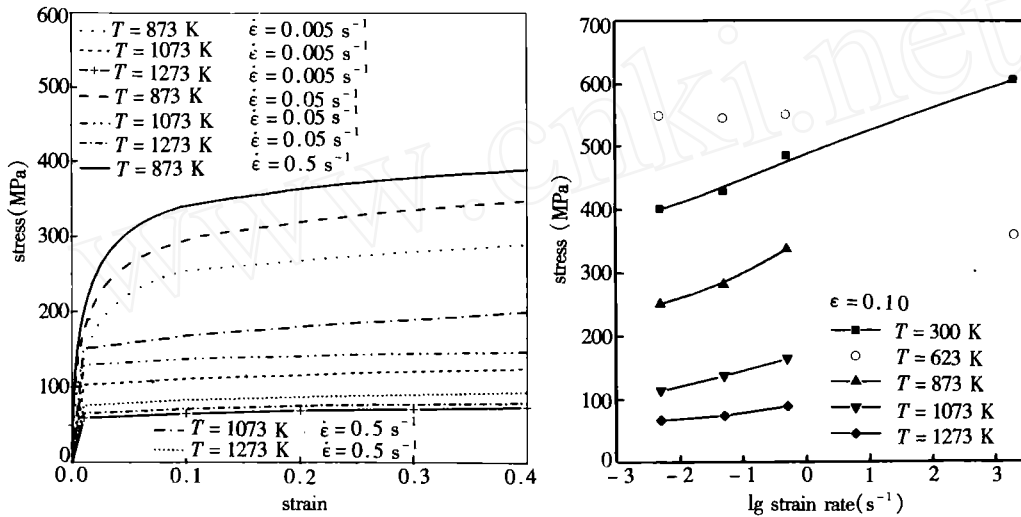


Fig.5 The strain-stress curves of 10 # steel under high temperature and low rate.

Fig.6 The strain rate sensitivity of 10 # steel at different temperatures.

$$\beta = \frac{\partial \sigma}{\partial \lg(\dot{\epsilon})} \tag{1}$$

where σ denotes the flow stress, $\dot{\epsilon}$ is the strain rate and β represents the strain rate sensitivity factor.

2.3 The History Effects of Temperature and Strain Rate

All the tests were conducted on Gleeble 1500 testing machine.

(1) Fixed the temperature rise rate (1000 K s^{-1}) and objective temperature (873 K or 1073 K), samples were stretched to a certain strain value with the deformation rate of $5 \times 10^{-3} \text{ s}^{-1}$, then, the tests were continued with higher strain rate of $5 \times 10^{-2} \text{ s}^{-1}$ until samples failed.

(2) Fixed the temperature rise rate (1000 K s^{-1}) and the strain rate ($5 \times 10^{-2} \text{ s}^{-1}$), when the tensile strain of sample was up to a certain value, the ambient temperature was changed suddenly (from 1073 K to 1273 K ; 873 K to 1273 K ; 300 K to 623 K) and the testing was resumed.

The experimental results were shown in Figs.7 and 8. The concept of temperature history effect

must be clarified in advance. It did not mean a pure heating and cooling procedure of a sample, but a coupling effect of temperature, deformation and loading. From Figs.7 and 8, it could be found that the history effect of strain rate was quite complex with the appearance of overshoot at 873 K. At the same time, a conclusion obtained from our experiments was that the history effects of temperature and strain rate were much weaker in comparison with the “up-to-date” strain rate effect and thermal softening effect.

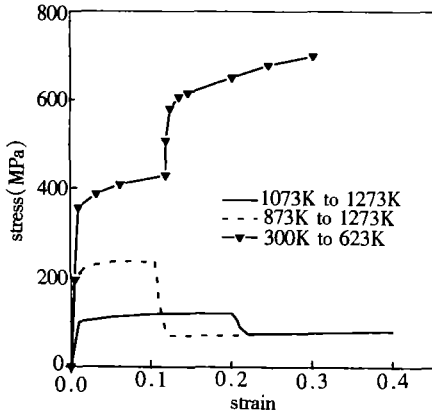


Fig. 7 The temperature jump testing results of 10 # steel.

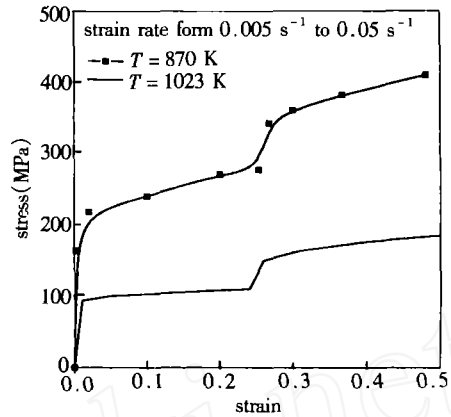


Fig. 8 The stress-strain curves recorded in the strain rate jump experiments.

III . SETTING UP OF CONSTITUTIVE LAW

As is mentioned in section one, the new constitutive law can be used to analyze the deformation of 10 # steel target under the irradiation of laser beam. So, the thermal mechanical characteristics of target irradiated by laser beam, high temperature rise rate and relatively wide variation ranges of temperature and strain rate must be incarnated in the constitutive law. In our experiments, it was found that the following factors should be considered in the setting up of the constitutive law. They are:

- (1) The effect of temperature rise rate;
- (2) Strain rate sensitivity and its history effect;
- (3) Dependence of yielding stress, strain hardening and strain rate hardening on temperature;
- (4) Temperature history effect.

Based on our experimental results and investigations of Anand^[2], Frost and Ashby^[1], a modified one-dimensional constitutive equation is presented as follows:

$$\dot{\epsilon}^p = \dot{\epsilon}_0^p \left\{ \sinh \frac{\sigma - \sigma_0 - Kl^{-1/2} - K_1 \epsilon^m - s}{C} \right\} \quad (2)$$

$$\dot{\epsilon}_0^p = A \exp\left(-\frac{Q}{RT}\right) \quad (3)$$

$$\dot{s} = [(C_1 + C_2 \ln z) \dot{\epsilon}^p] s \quad (4)$$

$$z = \dot{\epsilon}^p / \left[A \exp\left(-\frac{Q}{RT}\right) \right] \quad (5)$$

where σ is the flow stress, ϵ the strain, $\dot{\epsilon}^p$ the plastic deformation rate, T the temperature, R the Boltzmann constant, Q the strength index of obstacles, T_m the melting temperature, T_r the room temperature, T^* the relative temperature; K, l : the material constants in Hall-Petch equation, z the Zener

parameter. $C, A, Q, \sigma_0, K_1, m, n_1, C_1, C_2, C_r$ are constitutive parameters to be determined for the 10 # steel.

In Eq.(2), the hyperbolic sine function is adopted, because it can be changed to the exponential form automatically at a high strain rate and degrade to the power form at high temperature and lower strain rate. The above two functional forms can be used to describe the thermal activated glide and climb of dislocations, respectively. Usually, s is called the internal variable representing mathematically the variation of material microstructure. Theoretically, a single scale variable is in general not enough to contain such complex ingredients. In this paper, s is selected as an internal variable and a kind of compromise between accuracy and simplicity and is acceptable to monotonic loading.

For the convenience of engineering application, a simpler constitutive law has been developed based on our experiments and some rational hypotheses,

$$\sigma = (\sigma_0 + K_1 \epsilon^m)(1 - T^*) + Kl^{-1/2} + C \sinh^{-1} [(z)^{1/n_1}] \tag{6}$$

$$z = \dot{\epsilon}^p / \left[A \exp\left(-\frac{Q}{RT}\right) \right] \tag{7}$$

$$T^* = \frac{T - T_r}{T_m - T_r} \tag{8}$$

where $C, A, Q, \sigma_0, K_1, m, n_1$ are taken as a set of constitutive parameters.

In Eqs.(6-8), the effects of temperature rate and strain rate history are neglected. The effect of temperature rise rate is not shown in Eq.(6) because the temperature rise rate of target is about $10^3 - 10^7 \text{ Ks}^{-1}$, overrunning the turning point shown in Fig.1. However, all the experiments, for determining the constitutive law and parameters, should be conducted at high temperature rise rate. The reason for ignoring history effects is that they are not so important compared with those of "up-to-date" rate sensitivity and thermal softening, which is typical of BCC crystal structure steels.

The constitutive parameters in Eqs.(2-5) and (6-8) are determined by Marquardt nonlinear fitting technique and the results are shown in Table 3.

Table 3 The parameters in constitutive laws

type	$C(\text{MPa})$	$A(\text{s}^{-1})$	$Q(\text{J/mole})$	$\sigma_0(\text{MPa})$	$K_1(\text{MPa})$	m	n_1	C_1	C_2
2-5	18	0.27×10^{13}	0.22×10^6	60	110	0.27	4.8	-1.29	-0.23
6-8	18	0.27×10^{13}	0.22×10^6	60	410	0.25	4.8	/	/

From the SEM observation and the Ref.[3], in this constitutive law, $K = 22.4 \text{ N} \cdot \text{mm}^{-3/2}$, $l^{-1/2} = 7 \text{ mm}^{-1/2}$.

In order to obtain these constitutive parameters, 40 sets of data ($\sigma, \epsilon, \dot{\epsilon}_1, T_1, \dot{\epsilon}_2, T_2$) taken from various strain vs. stress curves (when $T = 623 \text{ K}, 873 \text{ K}, 1273 \text{ K}$; $\dot{\epsilon} = 0.05 \text{ s}^{-1}, 0.5 \text{ s}^{-1}$, respectively and jumping experiments of strain rate and temperature) are selected as input data in the fitting program.

In Figs.9-11, the experimental results and theoretically predicted values are compared at several different ambient temperatures and loading rates. The relatively small deviation between experimental and theoretical results shows the correctness of the constitutive form and parameters. Because some curves of strain vs. stress (when $\dot{\epsilon} = 10^3 \text{ s}^{-1}, T = 300 \text{ K}, 523 \text{ K}$; $\dot{\epsilon} = 0.05 \text{ s}^{-1}, 0.5 \text{ s}^{-1}, T = 1073 \text{ K}$; $\dot{\epsilon} = 0.005 \text{ s}^{-1}$) do not participate in the fitting but agree well with the theoretical curves, the pre-

dictive ability of the constitutive law is thus proven to be good to some extent.

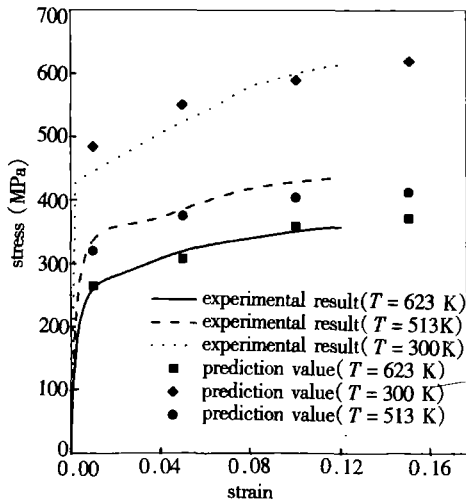


Fig. 9 Comparison of prediction values and experimental results (impact loading)

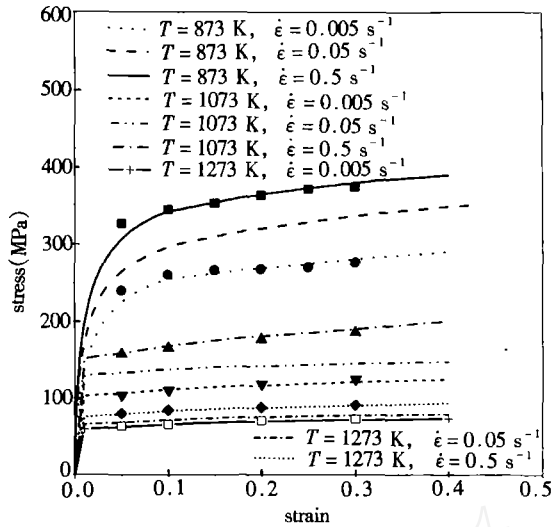


Fig. 10 Comparison of prediction values and experimental results (quasi-static loading). (Dispersed points represent the prediction values)

IV. CONCLUDING REMARKS

In this paper, a new one-dimensional constitutive law is presented to analyze the deformation and structure failure induced by laser beam for 10 # steel. This law was given on the basis of a series of systematic experiments and consideration of the deformation mechanism under different thermal and loading conditions. Compared with the model put forward by Anand^[2], the new constitutive law has the following main advantages.

- (1) Consideration of effects of temperature rise rate and microstructure of materials;
- (2) Including the temperature history effect;
- (3) Covering a wider range of strain rate.

However, some puzzling mechanical phenomena observed at the ambient temperature of 623 K do not seem to make sense with respect to the thermal softening and strain rate hardening. Hopes for an acceptable explanation will be pinned on future work.

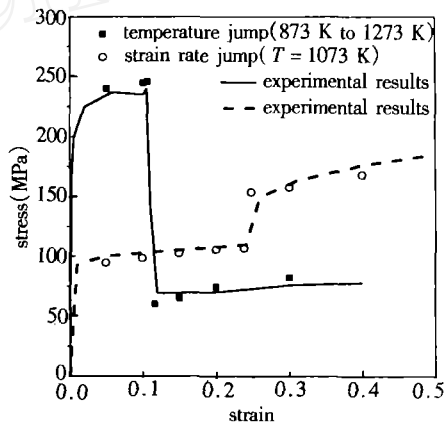


Fig. 11 The Comparison of prediction values and experimental results (temperature and strain rate jump testing, dispersed points represent the prediction values).

REFERENCES

[1] Frost, H.J. and Ashby, M.F., Deformation Mechanism Maps, Oxford Press, 1982.
 [2] Anand, L., Constitutive equation for hot working of metals, *Int. J. of Plasticity*, Vol. 1, 1985, 213.

- [3] Chan, L., Unified Equation for Creep and Plasticity, Miller, A. K. (eds.), Elsemer, New York, 1987, 273.
- [4] Johnson, G. R. and Cook, W. H., A constitutive model and data for metals subjected to large strains, In Proc. 7th Int. Symp. on Ballistics, The Hague, 1983, 541.
- [5] Perzyna, P., Advance in visco-plastic constitutive law, *Adv. in Appl. Mech.*, Vol. 9, 1966, 243 – 377.
- [6] Zerilli, F. J. and Armstrong, R. W., Dislocation-mechanics-based constitutive relations for materials dynamics calculation, *J. Appl. Phys.*, Vol. 61. No. 5, 1987, 1816.
- [7] Klepaczko, J. R., Discussion of microstructural effects and its modeling at high rate of strain, Proc. Int. Conf. Mech. Prop. of Mater. at High Rate of Strain, 1989.
- [8] Bodner, S. R. and Partom, Y., Constitutive equation for elastic-viscoplastic analysis strain-hardening materials, *J. Appl. Mech.*, Vol. 42, No. 2, 1975, 385 – 389.
- [9] Huang, C. G., Dynamic behaviors of several kind of metals and deformation and failure of structure irradiated by laser beam, the Ph. D. Dissertation of Institute of Mechanics, Chinese Academy of Sciences, 1996.
- [10] Klepaczko, J. R. and Duffy, J., History effects in polycrystalline FCC metals subjected to rapid changes in strain rate and temperature, *Arch. Mech.*, Vol. 34, 1982, 419.

www.cnki.net